Indian Journal of Engineering & Materials Sciences
Vol. 28, February 2021, pp. 55-63

Modeling of an active suspension system with different suspension parameters for full vehicle

Shailendra Kumar[a,b], Amit Medhavi[a,b] & Raghuvir Kumar[a,b]

[a]Department of Mechanical Engineering, Kamla Nehru Institute of Technology, Sultanpur, Uttar Pradesh 228 118, India

[b]Department of Mechanical Engineering, Motilal Nehru National Institute of Technology Allahabad, Prayagraj, Uttar Paresh 211 004, India

Received:18 January 2020 ; Accepted: 31 May 2020

An active suspension system attempts to overcome these compromises so as to provide the best performance for controlling the vehicle. A fully active suspension system aims to control the suspension over the full bandwidth, increase load carrying capacity, handling and ride quality. A model for vehicle's dynamics while using an active suspension system has been developed. The equations are cast in both the state space form and transfer function forms. To compare the ideal system and a real system, a comparative analysis is also performed by incorporating various sensing and actuation constraints such as time delay and discrete sampling. Simple PID as well as feed-forward controllers is designed and the response is simulated for various disturbances such as road excitations and those arising due to cornering. Parameter studies are also performed to assess the response to various suspension properties. The comparison of the active suspension with respect to the passive suspension indicates significant improvement in performance characteristics such as riding comfort, tendency to rollover and road traction. The studies on the effect of sensing and actuation constraints provide valuable insights into the use of low-cost and/or robust control system elements.

Keywords: Full vehicle model, State space equation, Passive and active suspension system, PID controller, Road profile, MATLAB and SIMULINK

1 Introduction

The objective of this study is to obtain a mathematical model for the full vehicle model's passive and active suspension systems and to create an active suspension control for a full vehicle model that is subject to excitation from a road profile using a PID control. Many of the car suspension systems still use passive components (use of the spring and damping coefficient at set levels only)[1]. Vehicle suspension systems are usually valued for their ability to provide good road handling and improved comfort for passengers. Passive suspensions provide a balance between these two contradictory requirements whereas an Active suspension lacks the ability to control the force actuators of suspensions directly. In this study the active suspension system for a complete vehicle model is synthesized based on PID power. For a given road profile the comparison between passive and active suspension system has been performed[2]. A comparison between Active and Passive suspension systems was carried out. The efficiency of this controller is calculated by the use of SIMULINK toolbox to perform computer simulations.

The use of active control system and semi-active control system in a vehicle suspension system has been the subject of substantial research since the late 1960s, see for example[3-8] and the references therein. Various theoretical and experimental studies have been carried out for semi-active vehicle models and active quarter-vehicle models form[9,10] but only a few studies have dealt with full-vehicle models. The controller design for an active suspension system of a full-vehicle model has first been investigated in[4], followed by work undertaken in[11]. Some simulation studies for semi active full-vehicle model has been undertaken in studies conducted from[12-15]. Applications using a neural network controller for quarter, half and full vehicle models have been discussed by researcher's from[16-18]. Four decoupled vehicle model using skyhook controllers have been investigated between the work from[19-21]. A Nonlinear Filter based observer structure has been proposed in[22], which takes the nonlinearities of the damper into account. Magnetorheological dampers have been investigated

*Corresponding author (E-mail: shailendra113.iitb@gmail.com)

through research work carried out from[23-26], which is a feedback control for a half and full-vehicle suspension system. An active suspension for the quarter, half and full vehicle model was developed in the studies conducted from[27-29]. Improved performance of the above models using a PID controller have been described in[30]. The full vehicle suspensions for passive and active models with PI controls has been discussed in[31] and PID controls in[32] were simulated using MATLAB/SIMULINK.

Based on the inference from the above literature review, the work carried out by researchers in the past is focused on linear quarter car, half car and nonlinear quarter car model for passive suspension. In this present work a linear full car model has been considered for investigation in addition, a comparative analysis has also been performed between hard and soft suspension systems. Simple PID as well as feed-forward controllers is designed and the response is simulated for various disturbances such as road excitations and those arising due to cornering.

2 Mathematical modeling of full vehicle model

Figure 1 shows the full-vehicle suspension framework model. The full-vehicle suspension model is characterized as a seven-degree (7-DOF) linear system. It comprises of a single jumping mass (car body) connected at each corner to four unsprung masses (front-left wheels, front-right wheels, rear-left wheels and rear-right wheels). The vehicle's body weight or sprung weight is free to heave, pitch, and roll while the unsprung weights are free to bounce vertically on the sprung weight. The suspensions between the sprung mass and the unsprung mass are modeled as linear viscous dampers and spring components, while the tires are considered simple linear springs without viscous damping. It has been assumed that all angles of pitch and roll are small. The model of full vehicle suspension system is represented as a dynamic equation and then its state-space formulation is obtained. The parameters used in the full vehicle suspension system in this study is given in Table 1.

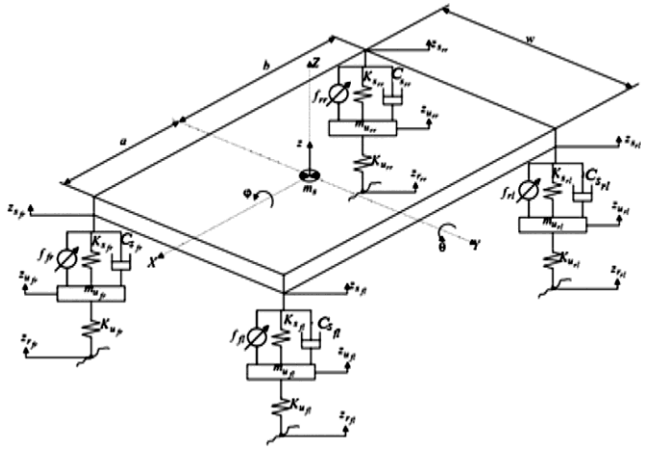

Fig. 1 — Active suspension model for full-vehicle system[33].

The dynamic equation of motion of full-vehicle system is given by.

$$M_s\ddot{z} = -(2K_{sf} + 2K_{sr})z - (2C_{sf} + 2C_{sr})\dot{z} + (2aK_{sf} - 2bK_{sr})\theta + (2aC_{sf} - 2bC_{sr})\dot{\theta} + K_{sf}z_{ufl} + C_{sf}\dot{z}_{ufl} + K_{sf}z_{ufr} + C_{sf}\dot{z}_{ufr} + K_{sr}z_{url} + C_{sr}\dot{z}_{url} + K_{sr}z_{urr} + C_{sr}\dot{z}_{urr} + F_{fl} + F_{fr} + F_{rl} \quad \ldots(1)$$

$$I_{yy}\ddot{\theta} = (2aK_{sf} - 2bK_{sr})z + (2aC_{sf} - 2bC_{sr})\dot{z} - (2a^2K_{sf} + 2b^2K_{sr})\theta - (2a^2C_{sf} + b^2C_{sr})\dot{\theta} - aK_{sf}z_{ufl} - aC_{sf}\dot{z}_{ufl} - aK_{sf}z_{ufr} - aC_{sf}\dot{z}_{ufr} + bK_{sr}z_{url} + bC_{sr}\dot{z}_{url} + bK_{sr}z_{urr} + bC_{sr}\dot{z}_{urr} - aF_{fl} - aF_{fr} + bF_{rl} + bF_{rr} \quad \ldots(2)$$

$$I_{xx}\ddot{\varphi} = -0.25w^2(2K_{sf} + 2K_{sr})\varphi - 0.25w^2(2C_{sf} + 2C_{sr})\dot{\varphi} + 0.5wK_{sf}z_{ufl} + 0.5wC_{sf}\dot{z}_{ufl} - 0.5wK_{sf}z_{ufr} - 0.5wC_{sf}\dot{z}_{ufr} + 0.5wK_{sr}z_{url} + 0.5wC_{sr}\dot{z}_{url} - 0.5wK_{sr}z_{urr} - 0.5wC_{sr}\dot{z}_{urr} + 0.5wF_{fl} - 0.5wF_{fr} + 0.5wF_{rl} - 0.5wF_{rr} \quad \ldots(3)$$

$$M_u\ddot{z}_{ufl} = K_{sf}z + C_{sf}\dot{z} - aK_{sf}\theta - aC_{sf}\dot{\theta} + 0.5wK_{sf}\varphi + 0.5wC_{sf}\dot{\varphi} - (K_{sf} + K_u)z_{ufl} - C_{sf}\dot{z}_{ufl} + K_u z_{rfl} - F_{fl} \quad \ldots(4)$$

Table 1 — Parameter values for full vehicle suspension[33].

Parameters	Value
Mass of vehicle body (sprung mass), M_s(kg)	1500
Roll axis moment of inertia of vehicle body,I_{xx} (kg-m^2)	460
Pitch axis moment of inertia of vehicle body,I_{yy}(kg-m^2)	2160
Mass of wheel (unsprung mass), Mu (kg)	59
Stiffness of vehicle body suspension spring for front, K_{sf}(N/m)	35000
Stiffness of vehicle body suspension spring for rear, K_{sr} (N/m)	38000
Tire spring stiffness, K_u (N/m)	190000
Front suspension damping, C_{sf} (N-s/m)	1000
Rear suspension damping, C_{sr}(N-s/m)	1100
Distance between front of vehicle and C.G. of sprung mass, a (m)	1.4
Distance between rear of vehicle and C.G. of sprung mass, b (m)	1.7
Width of sprung mass, *w* (m)	1.524
C.G. height, h_0 (m)	0.508
Distance between roll center and C.G. h_{roll}(m)	.3

$$M_u \ddot{z_{ufr}} = K_{sf} z + C_{sf} \dot{z} - aK_{sf} \theta - aC_{sf} \dot{\theta} - 0.5wK_{sf} \varphi - 0.5wC_{sf} \dot{\varphi} - (K_{sf} + K_u) z_{ufr} - C_{sf} \dot{z}_{ufr} + K_u z_{rfr} - F_{fr} \quad \ldots(5)$$

$$M_u \ddot{z_{url}} = K_{sr} z + C_{sr} \dot{z} + bK_{sr} \theta + bC_{sr} \dot{\theta} + 0.5wK_{sr} \varphi + 0.5wC_{sr} \dot{\varphi} - (K_{sr} + K_u) z_{url} - C_{sr} \dot{z}_{url} + K_u z_{rrl} - F_{rl} \quad \ldots(6)$$

$$M_u \ddot{z_{urr}} = K_{sr} z + C_{sr} \dot{z} + bK_{sr} \theta + bC_{sr} \dot{\theta} - 0.5wK_{sr} \varphi - 0.5wC_{sr} \dot{\varphi} - (K_{sr} + K_u) z_{urr} - C_{sr} \dot{z}_{urr} + K_u z_{rrr} - F_{rr} \quad \ldots(7)$$

3 Mathematical modeling for rollover

When a vehicle runs on a curved road, a centripetal force acts at the center of gravity of the vehicle given by Equation (8).

$$F_C = \frac{MV^2}{R} \quad \ldots(8)$$

where, Fc, M and V are centripetal force, total mass of vehicle and speed of the vehicle respectively. R is the curvature radius of the road. This centripetal force has a tendency to roll the vehicle over, which should be avoided. In this study an attempt has been made to analyze the rollover dynamics, thus an extra input to the vehicle has been given in addition to four wheels road input disturbances (as the road is being made to move rather than the vehicle). For creating a situation where the vehicle is running on a curved road and with a view to incorporate rollover, a centripetal force is applied as input to the system model. The roll moment acting on the vehicle due to this centripetal force is given by Equation (9).

$$M_{roll} = F_c h_{roll} \quad \ldots(9)$$

where, M_{roll} is the rolling moment acting on the vehicle and h_{roll} is the distance between the center of gravity of the vehicle and roll center. The rolling moment input is applied to the Equation (3) and the converted equation is given by Equation (10).

$$I_{xx} \ddot{\varphi} = -0.25w^2(2K_{sf} + 2K_{sr})\varphi - 0.25w^2(2C_{sf} + 2C_{sr})\dot{\varphi} + 0.5wK_{sf} z_{ufl} + 0.5wC_{sf} \dot{z}_{ufl} - 0.5wK_{sf} z_{ufr} - 0.5wC_{sf} \dot{z}_{ufr} + 0.5wK_{sr} z_{url} + 0.5wC_{sr} \dot{z}_{url} - 0.5wK_{sr} z_{urr} - 0.5wC_{sr} \dot{z}_{urr} + 0.5wF_{fl} - 0.5wF_{fr} + 0.5wF_{rl} - 0.5wF_{rr} + M_{roll} \quad \ldots(10)$$

4 State space formulation of full vehicle model

The state space variables for the full vehicle suspension model are assigned as in

Nomenclature

$y_1 = \dot{Z}$;	velocity (payload speed of sprung mass)
$y_2 = \dot{\theta}$;	pitch angular velocity
$y_3 = \dot{\varphi}$;	roll angular velocity
$y_4 = \dot{Z}_{ufl}$;	left-front wheel unsprung mass speed
$y_5 = \dot{Z}_{ufr}$;	right-front wheel unsprung mass speed
$y_6 = \dot{Z}_{url}$;	left-rear wheel unsprung mass speed
$y_7 = \dot{Z}_{urr}$	right -rear wheel unsprung mass speed
$y_8 = Z$;	heave position (ride height of sprung mass)
$y_9 = \theta$;	pitch angle
$y_{10} = \varphi$;	roll angle
$y_{11} = Z_{ufl}$;	left-front wheel unsprung mass displacement
$y_{12} = Z_{ufr}$;	right-front wheel unsprung mass displacement
$y_{13} = Z_{url}$;	left-rear wheel unsprung mass displacement
$y_{14} = Z_{urr}$;	right -rear wheel unsprung mass displacement

The state space equation is

$$\{\dot{y}\} = A\{y\} + B\{f\} + D\{r\} \quad \ldots(11)$$

where,

$\{y\}=[y_1 \ y_2 \ y_3 \ y_4 \ y_5 \ y_6 \ y_7 \ y_8 \ y_9 \ y_{10} \ y_{11} \ y_{12} \ y_{13} \ y_{14}]^T$; is the state vector

$\{r\} = [Z_{rfl} Z_{rfr} Z_{rrl} Z_{rrr} M_{roll}]^T$; is the road disturbance input vector

$\{f\} = [F_{fl} \ F_{fr} \ F_{rl} \ F_{rr}]^T$; is the control force input vector

A, B, and D are invariant coefficient

5 Transfer function formulation of the full car suspension system

The system transfer function for the full car suspension system obtained to study the open loop dynamics of the system and for the purpose of controller design for the active suspension system. In order to study the ideal system, a continuous time model and to study the realistic system, a discrete time model at different sampling frequencies is obtained and analyzed.

5.1 Continuous time model

The transfer function of the continuous time model for the full car suspension system is given in Equation (12). This transfer function relates each input to each output for a MIMO system and will be used latter to design the controller for the active suspension system.

$$\begin{pmatrix} Z_s(s) \\ \theta(s) \\ \varphi(s) \\ Z_{ufl}(z) \\ Z_{ufr}(z) \\ Z_{url}(z) \\ Z_{urr}(z) \end{pmatrix} = \begin{bmatrix} G_{11}(s) & G_{12}(s) & G_{13}(s) & G_{14}(s) & G_{15}(s) \\ G_{21}(s) & G_{22}(s) & G_{23}(s) & G_{24}(s) & G_{25}(s) \\ G_{31}(s) & G_{32}(s) & G_{33}(s) & G_{34}(s) & G_{35}(s) \\ G_{41}(s) & G_{42}(s) & G_{43}(s) & G_{44}(s) & G_{45}(s) \\ G_{51}(s) & G_{52}(s) & G_{53}(s) & G_{54}(s) & G_{55}(s) \\ G_{61}(s) & G_{62}(s) & G_{63}(s) & G_{64}(s) & G_{65}(s) \\ G_{71}(s) & G_{72}(s) & G_{73}(s) & G_{74}(s) & G_{75}(s) \end{bmatrix} \begin{pmatrix} Z_{rfl}(s) \\ Z_{rfr}(s) \\ Z_{rrl}(s) \\ Z_{rrr}(s) \\ M_{roll}(s) \end{pmatrix} \quad \ldots(12)$$

5.2 Discrete time model

The discrete time model of the full car suspension system is obtained and given by Equation (13). To see convergence of the discrete system the model is sampled at frequencies of 10 and 100Hz

$$\begin{pmatrix} Z_s(z) \\ \theta(z) \\ \varphi(z) \\ Z_{ufl}(z) \\ Z_{ufr}(z) \\ Z_{url}(z) \\ Z_{urr}(z) \end{pmatrix} = \begin{bmatrix} G_{11}(z) & G_{12}(z) & G_{13}(z) & G_{14}(z) & G_{15}(z) \\ G_{21}(z) & G_{22}(z) & G_{23}(z) & G_{24}(z) & G_{25}(z) \\ G_{31}(z) & G_{32}(z) & G_{33}(z) & G_{34}(z) & G_{35}(z) \\ G_{41}(z) & G_{42}(z) & G_{43}(z) & G_{44}(z) & G_{45}(z) \\ G_{51}(z) & G_{52}(z) & G_{53}(z) & G_{54}(z) & G_{55}(z) \\ G_{61}(z) & G_{62}(z) & G_{63}(z) & G_{64}(z) & G_{65}(z) \\ G_{71}(z) & G_{72}(z) & G_{73}(z) & G_{74}(z) & G_{75}(z) \end{bmatrix} \begin{pmatrix} Z_{rfl}(z) \\ Z_{rfr}(z) \\ Z_{rrl}(z) \\ Z_{rrr}(z) \\ M_{roll}(z) \end{pmatrix} \quad \ldots (13)$$

Due to symmetry, we have the following equalities for both cases:

$= G_{12};\ G_{13} = G_{14}; G_{21} = G_{22};\ G_{23} = G_{24};\ G_{31} = -G_{32}; G_{33} = -G_{34};$
$G_{31} = -G_{32}; G_{41} = G_{52}; G_{42} = G_{51}; G_{55} = -G_{45}; G_{63} = G_{74}; G_{64} = G_{73};$
$G_{43} = G_{54} = G_{61} = G_{72};\ G_{44} = G_{53} = G_{62} = G_{71};\ G_{75} = -G_{65};$

To study the convergence between continuous function and discrete function the transfer function $G_{11}(s)$ and $G_{11}(z)$ are plotted for sampling time 0.01 and 0.1 s both the magnitude and phase plots of these transfer functions are shown in Fig. 2.

In the frequency range of 1-40 rad/s for a sampling time of 0.01 s, the magnitude of the frequency response function of the discrete function is almost the same as that of the continuous function. For sampling time of 0.1 s there is some deviation of the discrete function's magnitude from that of the continuous system. There is also a significant deviation in the phase of the discrete system with respect to the continuous system, and this increases with the sampling time. The shorter the sampling time, the better the discrete function converges towards the continuous function. The similar trend can be seen in the Fig. 3 which plots transfer function G_{31}.

6 Controller design and response

6.1 Design of PID controller for active suspension system

In this study, the Ziegler-Nichols method is used to design the PID controllers. Transfer functions which are used obtain the critical gain (K_{cr}) and the critical time period (P_{cr}), and using these, the parameters of the PID controller are calculated.

6.2 Single input single output system

The transfer function for the system between the road disturbance applied to the front left tire and the body bounce is given as

$$G_{11}(s) = \frac{Z_s(s)}{Z_{rfl}(s)} = \frac{2147\ s^{11} + 2.145e5\ s^{10} + 3.344e7\ s^9 + 2.2e9\ s^8 + 1.61e11\ s^7 + 7.07e12\ s^6 + 2.698e14\ s^5 + 7.495e15\ s^4 + 1e17\ s^3 + 1.707e18\ s^2 + 9.291e18\ s + 1.022e20}{s^{14} + 84.05\ s^{13} + 1.844e4\ s^{12} + 1.073e6\ s^{11} + 1.186e8\ s^{10} + 4.7e9\ s^9 + 3.27e11\ s^8 + 8.06e12\ s^7 + 3.63e14\ s^6 + 4.314e15\ s^5 + 1.075e17\ s^4 + 7.074e17\ s^3 + 1.13e19\ s^2 + 3.389e19\ s + 3.727e20} \quad \ldots (14)$$

Bode plot of this open loop transfer function $G_{11}(s)$ is given in Fig. 4. The critical gain and frequency are given as:

$GM = -20 \log_{10} K_{cr}$ dB; $K_{cr} = 25.409$; $\omega_{cr} = 56.7$ rad/sec; $P_{cr} = 0.1108$ sec

where, gain margin (GM) is vertical distance in the magnitude Bode plot in dB (decibel) from the point where the gain crosses 0dB to the point where it crosses the phase crossover frequency (frequency at which the locus in phase Bode plot intersects the -180° axis).

The closed loop response when the PID parameters areK_p =25.409; K_i =0; K_d =0is given by Fig. 5. Sustained oscillations occur in response to a step input as expected using the Ziegler-Nichols criterion. The PID parameters according to the Ziegler-Nichols tuning rule and the transfer function of PID controller are given below.

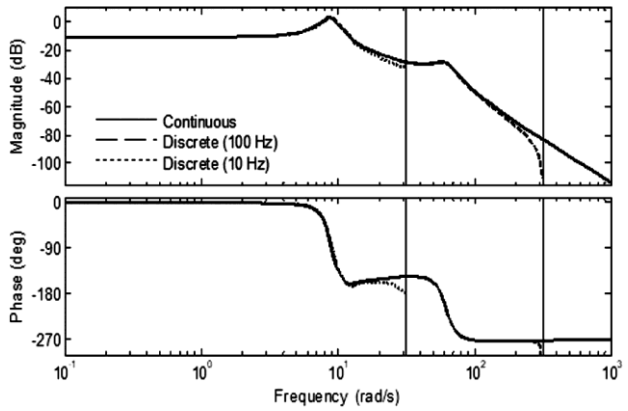

Fig. 2 — Magnitude and phase plot of $G_{11}(s)$ and $G_{11}(z)$.

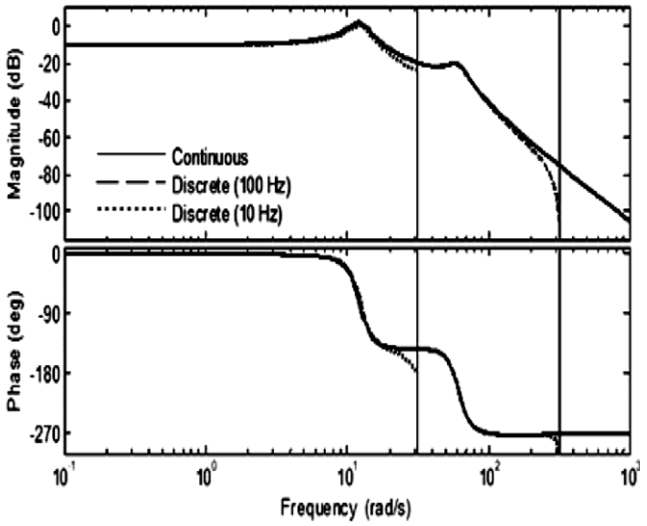

Fig. 3 — Magnitude and phase plot of $G_{31}(s)$ and$G_{31}(z)$.

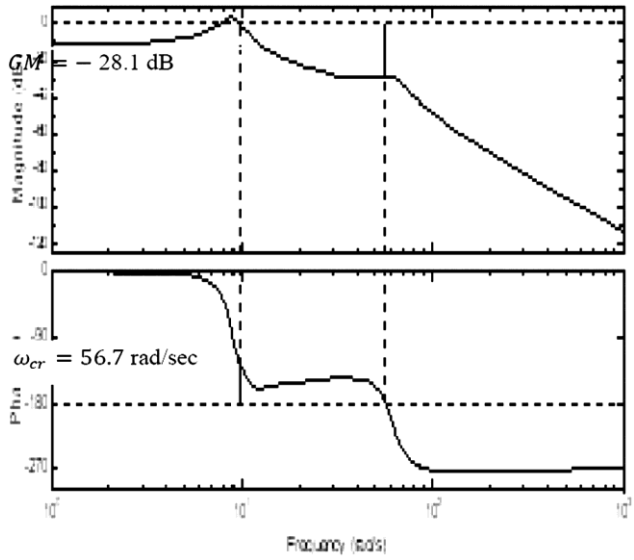

Fig. 4 — Bode plot for open loop transfer function $G_{11}(s)$.

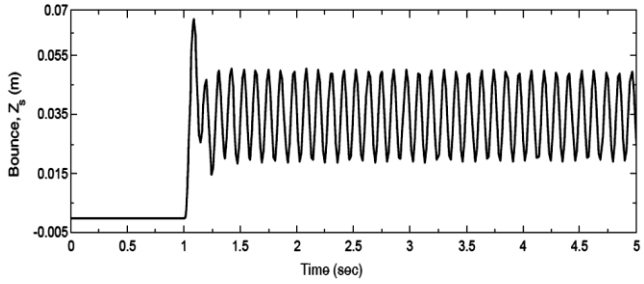

Fig. 5 — Close loop unit step input (K).

K_p =15.245; K_i =275.19; K_d =0.21

$$U_c(s) = \frac{0.21s^2 + 15.245s + 275.19}{s} \quad \ldots (15)$$

The closed loop transfer function is

$$CL_{11}(s) = \frac{G_{11}(s)}{1 + U_c(s)G_{11}(s)} \quad \ldots (16)$$

The (SISO) system $G_{11}(s)$ is simulated for a passive system and with a controller, and the responses are plotted in Fig. 6. The values of the PID parameters calculated by the Ziegler-Nichols method are only an intelligent guess, and a better response can be obtained by varying the parameters. The closed loop transfer function is plotted in Fig. 7. After applying the PID controller, the gain margin decreases employing that the system becomes more stable.

7 Results and Discussion

7.1 Road profile

Road profile irregularities in nature were classified as smooth, rough minor, or rough. A smooth road profile means a single bump road disturbance. The rough minor and rough road profiles are characterized by the uniform height of the bump and uniform height of the bump[3].

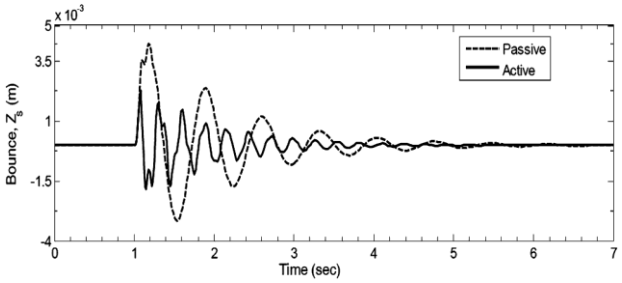

Fig. 6 — Vertical amplitude versus time for the SISO system $G_{11}(s)$.

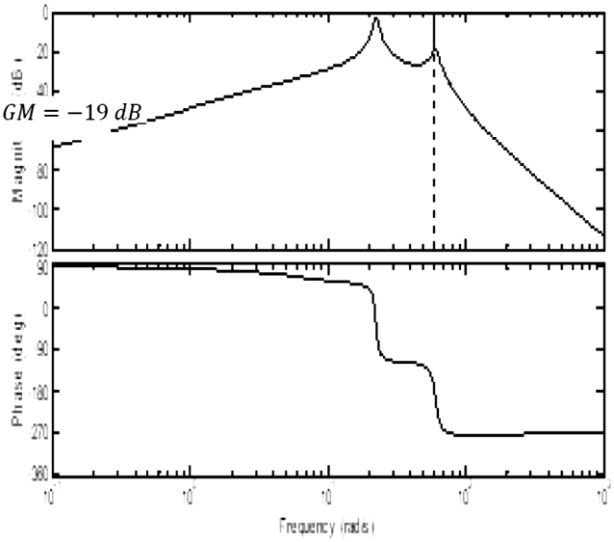

Fig. 7 — Bode plot for closed loop transfer function $CL_{11}(s)$.

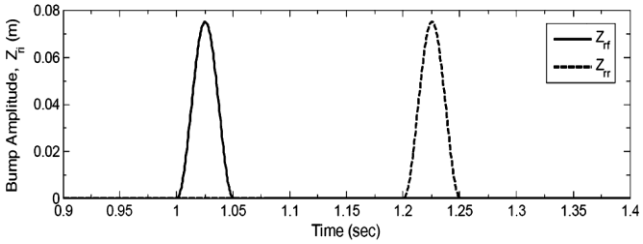

Fig. 8 — Sinusoidal bump road input disturbance time histories for the front and rear wheels.

$$Z_{rf} = \begin{cases} \frac{a_0}{2}\left(1 - \cos\left(\frac{2\pi V t_f}{\lambda_0}\right)\right) 1 \le t_f \le 1 + \frac{\lambda_0}{V} \\ 0 \; Otherwise \end{cases} \quad \ldots (16)$$

$$Z_{rr} = \begin{cases} \frac{a_0}{2}\left(1 - \cos\left(\frac{2\pi V t_r}{\lambda_0}\right)\right) t_{r0} \le t_r \le t_{r0} + \frac{\lambda_0}{V} \\ 0 \; Otherwise \end{cases} \quad \ldots (17)$$

In this study two types of road input excitation are given namely left wheel input and a speed breaker respectively to study the behavior. For the left wheel input, a single bump is given to the front-left and rear tires. For the speed breaker input, both or either of the front or rear tires hit the bump. A graphical representation of the road profile is given by Fig. 8.

The profile road bump inputs for the front wheels and rear wheels can be given by the following equations[4].

where, a_0 is the bump amplitude, V is the vehicle forward velocity, λ_0 is the disturbance wavelength, t is the simulation time and subscripts rf and rr denote the road-front and road-rear wheel inputs to the suspension respectively.

tr_0 = 1+td where td is the time delay between the front and rear wheel, written as:

$$t_d = \frac{a+b}{V} \quad \ldots(18)$$

For this study

a_0 = 0.075m; λ_0 = 0.775m and V = 15.5m/s

There are various parameters which have a strong effect on the performance of the active suspension system when this concept is brought into realization. In this study, to analyze the impact of the parameters like suspension stiffness, static stability factor, time delay and discrete time sampling on the active suspension system are presented.

7.2 Effect of suspension stiffness

In this section a comparative analysis is performed between hard and soft suspension systems. In the analysis road bump to left wheel used as the disturbance. The hard and soft suspension system is defined by the suspension travel. Travel can be defined as the distance from the bottom of the suspension stroke (when the vehicle is suspended and the wheel is freely suspended) to the top of the suspension stroke (when the wheel of the vehicle can no longer move upwards towards the vehicle)[6]. An example of hard and soft suspension parameters is given in Table 2.

Figure 9 (a) and (b) depict the passive and active responses for bounce with soft and hard suspension systems respectively. The passive response shows that there is only a small difference in amplitude of bounce, though the settling time is almost double with the soft suspension compared to the hard. The active response shows that the amplitude of bounce with the soft suspension is lower and the settling time is almost same with both suspension systems which make an active suspension system to prefer soft suspension stiffness to achieve lower body bounce.

Figure 10 (a) and (b) depict the passive and active responses for pitch with soft and hard suspension systems respectively. The passive response shows that there is only a small difference in the pitching angle though the settling time is almost double for the soft

Table 2— Hard and soft suspension system parameters.

Suspension parameter	Hard Suspension	Soft Suspension
Front wheel suspension damping, C_{sf}(N-s/m)	1000	300
Rear wheel suspension damping, C_{sr}(N-s/m)	1100	330
Front wheel suspension spring stiffness, K_{sf} (N/m)	35000	20000
Rear wheel suspension spring stiffness, K_{sr}(N/m)	38000	20500

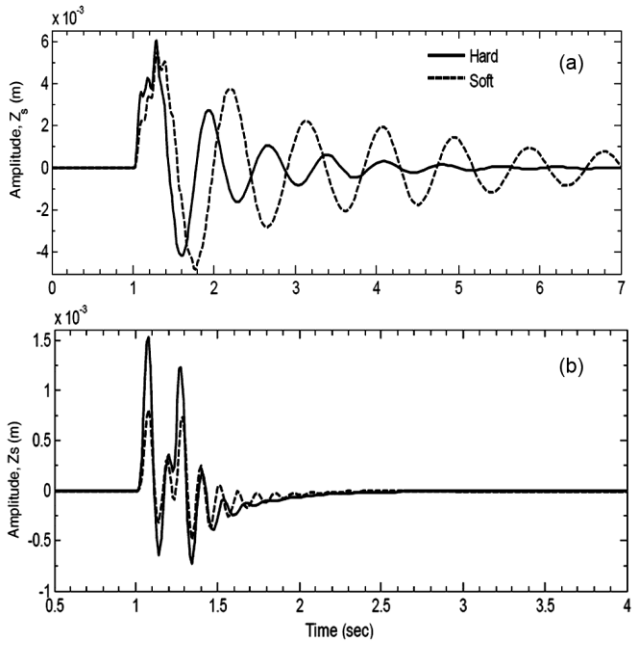

Fig. 9 — Vertical displacement versus time for both front and rear road inputs (a) passive system and (b) active system.

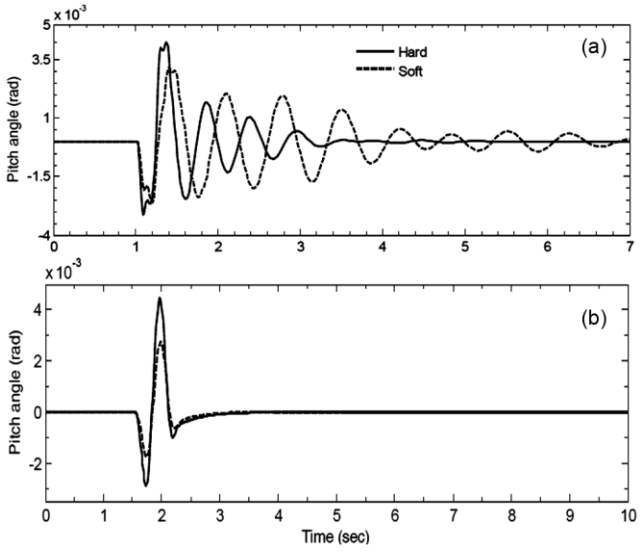

Fig. 10 — Pitch response for both front and rear road inputs (a) passive system and (b) active system.

suspension compared to the hard. The active response shows that the pitch angle is almost half with the soft suspension compared to that of hard and the settling time is almost same which make soft suspension is preferred over hard suspension stiffness to achieve lower pitch.

Figure 11 (a) and (b) depict the passive and active responses for roll with soft and hard suspension systems respectively. The passive response shows that there is only a difference in the roll angle though the settling time is almost double for the soft suspension compared to the hard.The active response shows that the roll angle is almost half with soft suspension to that of the hard and the settling time is almost same which make an active suspension system to prefer soft suspension stiffness to achieve lower roll on straight road drive.

Figure 12 (a) and (b) depict the passive and active responses for roll of soft and hard suspension system respectively during cornering. The passive response shows that the roll angle of the soft suspension system is 1.7 times that of hard suspension and the settling time is also more. The active response shows that both systems have almost same response. Hence during cornering, suspension stiffness does not affect too much on roll response. From the above discussions it seen that a soft suspension is preferred for straight road drive and a hard one for cornering.

7.3 Static stability factor (SSF)

The static stability factor is a measure of the vehicle's tendency to rollover and hence for this study, the curved road is used as the disturbance input for cornering. The system parameters for two vehicles having different SSF are given in Table 3.

Figure 13 (a) and (b) depict the roll response for the vehicles with different SSF. It can be seen that vehicle having a higher SSF has smaller roll angle than the vehicle having lower SSF. Hence as expected, the vehicle having a Higher SSF is less vulnerable to rollover.

7.4 Effect of control action on the system

In an ideal system the control action occurs continuously and instantly. In reality though, the action occurs at discrete time intervals due to sampling, there is some time delay between sensing the signal and performing corrective action via controller through the actuator. The effects of these limitations of a real system are simulated to analyze the effect of time delay and discrete time.

7.5 Effect of time delay

In the simulation that follows a time delay of 0.02s is assumed between sensing of the generated signal and the corrective action by the actuator via the control signal. A left wheel road bump disturbance is given as input responses are shown in Fig. 6. Figure 14 depicts the response for the bump road disturbance for the left wheel and Fig. 15 depicts for the curve road input respectively with the systems having controller time delay. It can be seen that the suspension system with delay has inferior response

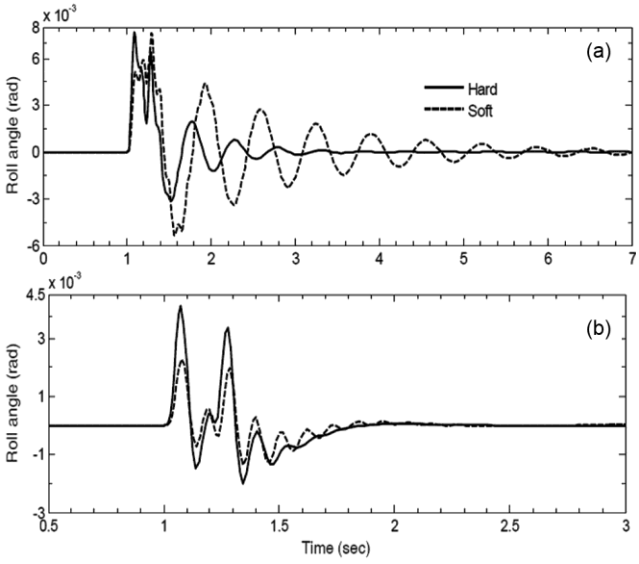

Fig. 11 — Roll response for both front and rear road inputs (a) passive system and (b) active system.

Table 3 — Parameters for different SSF[15].

SSF	1.5	1
Track width, t_W (m)	1.524	1.42
C.G. height, h_0 (m)	0.508	0.736
Distance between roll center and C.G (m)	0.3	0.4

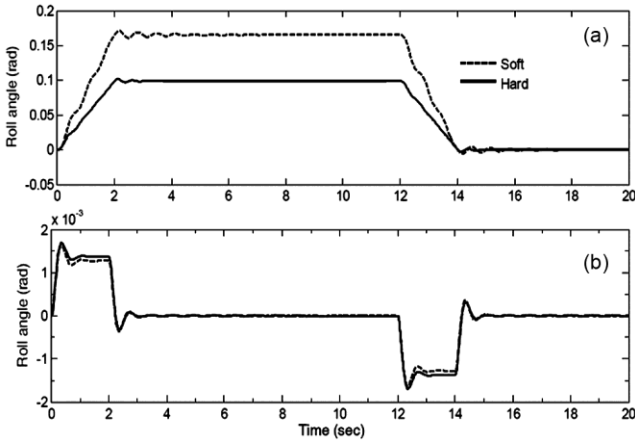

Fig. 12 — Roll response during cornering for both front and rear road inputs (a) passive system and (b) active system.

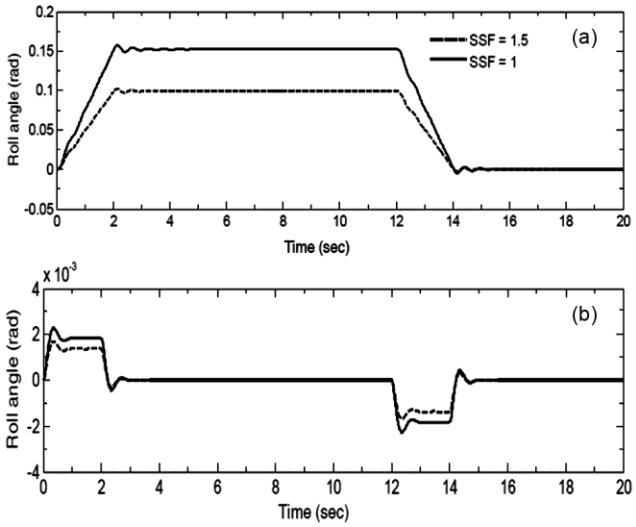

Fig. 13 — Roll Response for vehicles with different SSF (a) passive system and (b) active system.

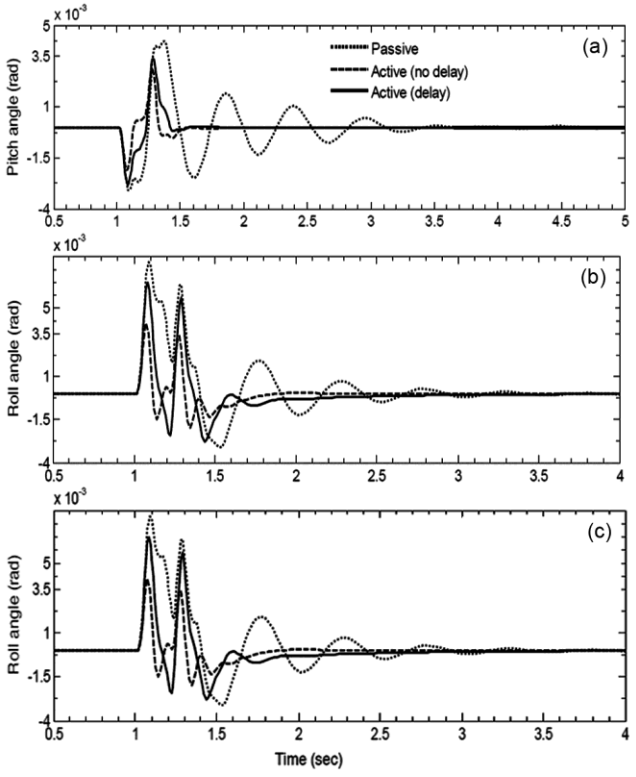

Fig. 14 — Effect of time delay on systems response for both front and rear road inputs (a) vertical amplitude, (b) pitch and (c) roll.

than the suspension system without time delay. The response of the system without delay shows theoretical limit of the correction that can be achieved by a specific controller-equipped suspension system, while the response of the system with delay shows what can possibly be achieved in actual practice. Hence while designing an active suspension system

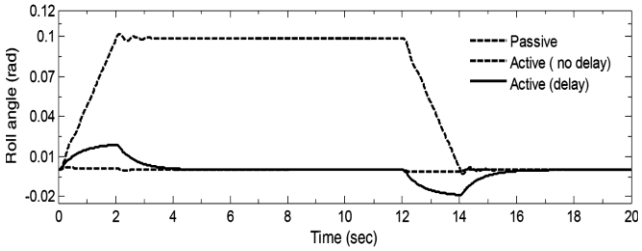

Fig. 15 — Vertical Displacement of the system with the effect of discrete time

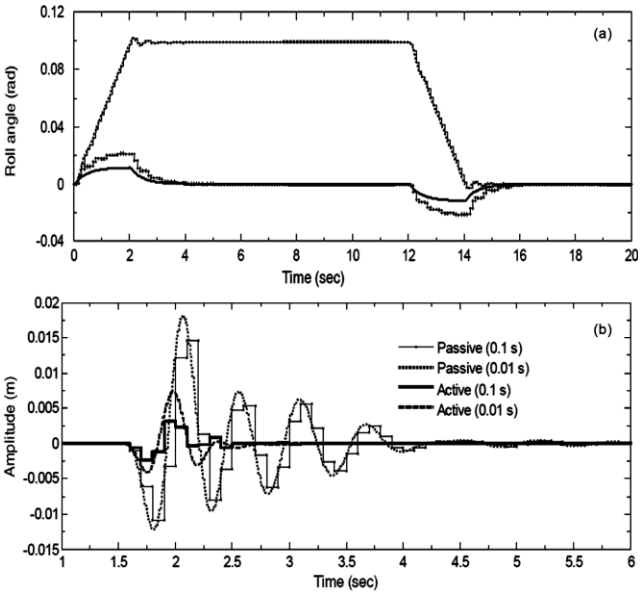

Fig. 16 — Roll response of the system with the effect of discrete time for both front and rear road inputs.

different element like the sensor, controller and actuator should be selected such that there is minimum time delay.

7.6 Effect of sampling

A real control system operates in discrete domain that is dependent on the sampling frequency. In order to compare the continuous and discrete systems, it is modeled for two sampling times, 0.1 and 0.01s. The simulated responses with curved road profile as the road input are shown in Fig. 16 (a).

The figure shows that the response of the discrete system having sampling time of 0.01 s is very similar to that of the continuous system. However, the response for a system with sampling time 0.1 s degrades significantly compared to the continuous response. Therefore, the less the sampling time, better the discrete system converges toward the continuous system and the better the response. A similar trend can be seen in Fig. 16 (b), where vertical amplitude is shown.

8 Conclusions

The current study involves the investigation of a linear full car model; a comparative analysis between hard and soft suspension systems has also been carried out. A simple PID as well as the feed-forward controller has been designed and its response has been simulated for various disturbances arising due to road excitations and cornering of the vehicle. Form the results obtained during the study the improvement in the performance of the vehicle while running on a straight road and when subjected to bump disturbances may be summarized as follows: The active response shows that for soft suspension the pitch angle and roll angle is almost half as compared to that obtained when a hard suspension is used while the settling time is almost the same, this makes the soft suspension system more preferable over the hard suspension. Thus, a soft suspension is preferred while driving on a straight road as compared to a hard suspension which is preferred during cornering of the vehicle. For vehicles having higher SSF the roll angle is small as compared to vehicles having lower SSF, hence the vehicle having Higher SSF is less vulnerable to rollover. The response of the system without delay shows theoretical limit of the correction that can be achieved by a specific controller-equipped suspension system, while the response of the system with delay shows what can possibly be achieved in actual practice. On reducing the sampling time, the discrete system converges to the continuous system, thus giving better response. From the results of the study, it is established that an active suspension system is capable of providing good ride comfort, safety and is more efficient in rollover prevention.

Acknowledgement

Research Funded through World Bank Technical Education Quality Improvement Programme Phase Third (WB TEQIP-III) (Grant No/Scheme No- 2038) Projectof Kamla Nehru Institute of Technology, Sultanpur-228118, Uttar Pradesh, India.

References

1 Dong X, Zhao D, Han B & Chenghao, *J Mech Sci Technol*, 30 (2016) 2769.
2 Darus R & Sam Y Md, *5th Int Colloquium on Signal Proc Application*, 978-1-4244-4152-5 (2009) 13.
3 Thompson G, *Proc of the Inst of Mech Eng*, 185 (1970-1971) 553.
4 Chalasani R M, *ASME, App Mech Division*, 80 (1986) 205.
5 Hrovat H, Margolis D & Hubbard M, *ASME, J Dyn Syst Meas Control*, 110 (1988) 288.
6 Appleyard M & Wellstead P E, *Control Theory Appl*, 142 (1995) 123.
7 Hayakawa K, Matsumoto K, Yamashita M, Suzuki Y, Fujimori K & Kimura H, *IEEE Trans Proc 32nd IEEE Conf Decis Control*, 44 (1999) 392.
8 Choi B, Lee H S & Park Y P K, *Veh Syst Dyn*, 38 (2002) 341.
9 Giorgetti N, Bemporad A, Tseng H E & Hrovat D, *Proc of the IEEE I Symp on Ind Electron*, 0-7803-8738-4 (2005) 391.
10 Yi K & Song B S, *Corresp author Sch Mech Eng*, 213 (1999) 293.
11 Smith M C, *IEEE Trans on Control Syst Technol*, 10 (2002) 393.
12 Nguyen MQ, Canale M, Sename O & Dugard L, 55*th IEEE Conf on Decis and Control (CDC)*, 978-1-5090-1837-6 (2016) 721.
13 Fang Z, Shu W, Du D, Xiang B, He Q & He K I, *Work Automob Power Energy Eng, Proc Eng*, 16 (2011) 428.
14 Dezasse M F & Brembeck J, *IFAC-Papers Online*, 49 (2016) 432.
15 Jahromi A F & Zabihollah A, *Proceedings of 2010 IEEE/ASME I Conf on Mech and Embedded Sys and Appl*, 978-1-4244-7101-0 (2010) 522.
16 CsekőL H, Kvasnica M & Lantos B, *IEEE Transa on Control Syst Technol*, 23 (2015) 1736.
17 Pang H & Liu F, *Neurocomputing*, 306 (2018) 130.
18 GucluR & Gulez K, *Math Comput Model*, 47 (2008) 1356.
19 Hu Y, Chen M Z Q & Sun Y, *J Sound Vib*, 405 (2017) 34.
20 Ahmadian M, Song X & Southward S C, *ASME J Vib Acoust*, 126 (2004) 580.
21 Sandhu F,Selamat H & Sam Y MD, *10th Asian Control Conf*,978-1-4799-7862-5 (2015) 1.
22 Koch G, Kloiber T, Pellegrini E & Lohmann B, *Am Control Conf Marriott Waterfront, Balt, MD, USA*, 978-1-4244-7427-1 (2010) 4576.
23 Choi S B, Lee H S & Park Y P, *Veh Syst Dyn Int J Veh Mech Mobil*, 38 (2010) 341.
24 Prabakar R S, Sujatha C & Narayanan S, *J Sound Vib*, 332 (2013) 2191.
25 Yu M, Dong X M, Choi S B & Liao CR,*J Sound Vib*, 319 (2009) 753.
26 Yerrawar R N & Arakerimath R R, *Mater Today Proc*, 4 (2017) 9294.
27 Mohite A G & Mitra A C, *Mater Today Proc*, 5 (2018) 4317.
28 Singh D, *Simul Model Pract Theory*, 89 (2018) 100.
29 Sharma S K, Pare V, Chouksey M & Rawal B R, *Proc Technol*, 23 (2016) 171.
30 Haemers M & Derammelaere S, *IFAC-Papers Online*, 51 (2018) 1.
31 Geweda A E, El-Gohary MA, El-Nabawy AM & Awad T, *Alexandria Eng J*, 56 (2017) 405.
32 Tandel A, Deshpande A R, Deshmukh S P & Jagtap K R, *Proc Eng*, 97 (2014) 1274.
33 Ikenaga S, Lewis F L, Campos J & Davis L, *Proc 2000 Am Control Conf*, 6 (2000) 4019.